Experimental and Molecular Dynamics Studies of Dysprosium(III) Salt Solutions for a Better Representation of the Microscopic Features Used within the Binding Mean Spherical Approximation Theory

Alexandre Ruas,[†] Philippe Guilbaud,[†] Christophe Den Auwer,[†] Christophe Moulin,[‡] Jean-Pierre Simonin,[§] Pierre Turq,[§] and Philippe Moisy*,[†]

DEN/DRCP/SCPS, CEA-Valrhô Marcoule, BP 17171, 30207 Bagnols-sur-Cèze Cedex, DEN/DPC/SECR/LSRM, CEA-Saclay, Bât 391, BP 91191 Gif sur Yvette, Cedex, and Laboratoire LI2C (UMR 7612), Université Pierre et Marie Curie-Paris 6, Boîte No. 51, 4 Place Jussieu, 75252 Paris Cedex 05, France

Received: February 15, 2006; In Final Form: June 2, 2006

This work is aimed at a predictive description of the thermodynamic properties of actinide(III) salt solutions at high concentration and 25 °C. A new solution of the binding mean spherical approximation (BIMSA) theory, based on the Wertheim formalism, for taking into account 1:1 and also 1:2 complex formation, is used to reproduce, from a simple procedure, experimental osmotic coefficient variation with concentration for three binary salt solutions of the same lanthanide(III) cation: dysprosium(III) perchlorate, nitrate, and chloride. The relevance of the fitted parameters is discussed, and their values are compared with available literature values. UV–vis/near-IR, time-resolved laser-induced fluorescence spectroscopy experiments, and molecular dynamics (MD) calculations were conducted for dilute to concentrated solutions (ca. 3 mol·kg⁻¹) for a study of the microscopic behavior of $DyCl_3$ binary solutions. Coupling MD calculations and extended X-ray absorption fine structure led to the determination of reliable distances. The MD results were used for a discussion of the parameters used in the BIMSA.

Introduction

For the improvement of the spent nuclear fuel reprocessing, actinide salt solution thermodynamic properties constitute essential data. A better control of the separation process by means of liquid–liquid extraction equilibria requires the knowledge of actinide activity coefficients, up to high concentration.[1]

As compared to that of any other element, the measurement of actinide (An) thermodynamic properties is a difficult task due to their radioactivity. Also, the number of oxidation states (from +III to +VI) and structural forms (an actinide(III/IV) is in the aquo form, whereas an actinide(V/VI) is in the "yl", AnO_2^{n+}, form) strengthens the difficulty of measuring the properties of an element in a given state and increases the number of required data. As a consequence, thermodynamic data on actinide salt solutions are rather scarce, especially at high concentration.[2] Therefore, a theory capable of predicting actinide thermodynamic properties, and complete experimental data, would be welcome.

This work is aimed at solving this issue in the case of actinide-(III) (An(III)) salt aqueous solutions. Actually, this type of system is probably the most convenient one for predictive applications because it can be based on the properties of lanthanide(III) (Ln(III)) salts, which are commonly regarded as actinide(III) salt analogues[2] and whose thermodynamic properties (e.g., osmotic coefficients) have been widely and accurately studied in the past.[3–10] However, because they are highly charged (+III) cations, forming weak complexes[11] in the case

of nitrates and chlorides, the thermodynamic properties of lanthanides(III) and their derivative salts are difficult to describe within a model. Various thermodynamic models exist for ionic solutions, such as the Brønsted–Guggeheim–Scatchard theory[12–14] and Pitzer method.[15] The latter is accurate up to high concentration (typically up to 6 mol·kg⁻¹ [16]). Nevertheless, it essentially makes use of semiempirical parameters, which is an issue for predictive applications.

In contrast, the binding mean spherical approximation (BIMSA) theory, derived from the Wertheim formalism, seems a promising alternative. We have seen in previous work that the BIMSA theory could reproduce osmotic coefficients for lanthanide(III) perchlorates and for the partially associated electrolytes lanthanide(III) chloride and nitrate salts. The fit could be done up to high concentration with the use of a restricted number of adjustable parameters that have some physical meaning.[17,18]

However, the previously obtained results raised some questions regarding the theory, so the formerly used model took into account only 1:1 complex formation ($K_1°$),[17] while the 1:2 complex ($K_2°$) can be expected for lanthanide(III) and actinide-(III) chlorides and nitrates at high concentration.[19–25] It was also observed that obtaining a common value for the parameter $\sigma_+^{(0)}$ (cation diameter at infinite dilution) in the case of perchlorate, chloride, and nitrate salts of the same lanthanide-(III) cation[17] was a source of difficulties. Finally, the BIMSA parameters $\sigma_+^{(0)}$ and $\sigma^{(1)}$ (parameter of the hydrated cation size decrease with concentration), despite being interpreted in terms of hydration, which includes a first hydration sphere and also a second hydration sphere,[26] seemed to suffer from a lack of direct comparison with literature structural data.

Considering these remarks, the purpose of the paper is threefold. Focus is on Dy(III) since its derivative salts can be

* To whom correspondence should be addressed. E-mail: philippe.moisy@cea.fr.
† CEA-Valrhô Marcoule.
‡ CEA-Saclay.
§ Université Pierre et Marie Curie-Paris 6.

Lanthanide and Actinide Solution Thermodynamics

J. Phys. Chem. A, Vol. 110, No. 41, 2006 **11771**

studied by complementary spectroscopic approaches, namely UV−vis−near-IR absorption spectroscopy, time-resolved laser-induced fluorescence spectroscopy (TRLFS), and extended X-ray absorption fine structure (EXAFS).

First, a modified BIMSA theory, taking into account 1:1 and 1:2 complex formation, is used to represent experimental data[3,4,7] for the osmotic coefficient of dysprosium perchlorate, chloride, and nitrate. Improvements brought about by this new model and comparison of our fitted parameter values with literature data are discussed. Second, we study the structure of the first hydration shell of aqueous $DyCl_3$ solutions, up to high concentrations, by using UV−vis−near-IR absorption spectroscopy, TRLFS, and EXAFS. Last, because of the difficulty of obtaining experimental data for the second hydration sphere of a cation, molecular dynamics (MD) calculations are reported on the same $DyCl_3$ solution at various concentrations.

Interpretation of the obtained structural information from the different methods and discussion in terms of the parameters $\sigma_+^{(0)}$ and $\sigma^{(1)}$ are given. A possibility for minimizing the number of adjustable parameters and using input data from different techniques in the BIMSA model is discussed.

Experimental Protocol

Seven $DyCl_3$ solutions were prepared by dissolving weighed quantities of $DyCl_3 \cdot 6H_2O$ Aldrich salt (solid S) of purity 99.9% in deionized water. X-ray powder diffraction of the commercial salt, obtained with an INEL CPS 120 diffractometer using Cu $K\alpha_1$ radiation isolated by a germanium monochromator, confirmed a stoichiometry of $DyCl_3 \cdot 6H_2O$ as in ref 27. For each dysprosium chloride solution, diluted Prolabo Normapur hydrochloric acid was added to maintain a slightly acidic pH value (of about 3) and to avoid dysprosium hydrolysis. The added proportion of hydrochloric acid was weak enough to consider that our $DyCl_3$ solutions are binary solutions. The concentrations of dysprosium chloride solutions were verified from UV−vis spectra of each sample, diluted in $HClO_4$, 1 mol·L^{-1}. Conversion from molar scale to molal scale was done using dysprosium chloride density data from ref 28.

The studied $DyCl_3$ solution concentrations are (solution A) 0.10 mol·L^{-1} (0.10 mol·kg^{-1}), (solution B) 0.50 mol·L^{-1} (0.51 mol·kg^{-1}), (solution C) 1.00 mol·L^{-1} (1.03 mol·kg^{-1}), (solution D) 1.50 mol·L^{-1} (1.57 mol·kg^{-1}), (solution E) 2.00 mol·L^{-1} (2.14 mol·kg^{-1}), (solution F) 2.50 mol·L^{-1} (2.73 mol·kg^{-1}), and (solution G) 3.00 mol·L^{-1} (3.36 mol·kg^{-1}).

Ternary dysprosium perchlorate−perchloric acid solutions were prepared from a commercial Aldrich solution ([Dy(ClO$_4$)$_3$] = 1.28 mol·L^{-1} and [Dy(ClO$_4$)$_3$]/[HClO$_4$] close to 2). Samples of this commercial solution were diluted or concentrated to give three ternary dysprosium perchlorate−perchloric acid solutions: (solution X) [Dy(ClO$_4$)$_3$] = 0.64 mol·L^{-1}, (solution Y) [Dy(ClO$_4$)$_3$] = 1.28 mol·L^{-1}, and (solution Z) [Dy(ClO$_4$)$_3$] = 2.56 mol·L^{-1}.

UV−vis−near-infrared absorption spectrophotometry measurements were performed using a dual-beam, double-monochromator spectrophotometer (Shimadzu UVPC 3101) for dysprosium salt solutions, using Hellma Suprasil quartz vessels (optical path length of 0.1 or 1 cm). The spectra were recorded at room temperature, between 300 and 1200 nm. A diffuse solid-state reflectance spectrum was obtained using a Shimadzu ISR-3100 UV−vis−near-IR integrating sphere.

For the TRLFS measurements, a Nd:YAG laser (model Minilite, Continuum) operating at 266 nm (quadrupled) and delivering about 2 mJ of energy in a 4 ns pulse with a repetition of about 15 Hz was used as the excitation source. The laser

beam was directed into the 4 mL quartz cell of the spectrofluorometer "FLUO 2001" (Dilor, France). The radiation coming from the cell was focused on the entrance slit of the polychromator (focal length 50 cm and 1 mm slit widths). Taking into account dispersion of the holographic grating (300 g/mm, blaze 500 nm) used in the polychromator, the measurement range extends approximately 200 nm into the visible spectrum with a resolution of 1 nm. The detection was performed by an intensified photodiode (1024) array cooled by the Peltier effect (−20 °C) and positioned at the polychromator exit. Recording of the spectra was performed by integration of the pulsed light signal given by the intensifier. The integration time, adjustable from 1 to 99 s, allows for variation in the detection sensitivity. Logic circuits, synchronized with the laser shot, allow the intensifier to be active with a determined time delay (from 0.1 to 999 μs) and during a determined aperture time from 0.5 to 999 μs.

EXAFS data for solutions A (0.1 mol·L^{-1}) and G (3.0 mol·L^{-1}) were recorded at the European Synchrotron Radiation Facility, on BM29, in transmission mode. The ring was operated at 6 GeV with a nominal current of 200 mA. The line is equipped with a fixed-exit double-crystal Si(311) helium-cooled monochromator. Higher harmonics were rejected by two Si mirrors (cutoff at 11 keV). Energy calibration of the monochromator was achieved at the Fe K edge (7112 eV). Data treatment was carried out using Athena code.[29] Background and atomic subtraction was done with the AUTOBK procedure. Experimental EXAFS data in $k^3\chi(k)$ between 1.9 and 14.0 Å^{-1} were fitted in R space (Kaiser−Bessel window) without any filtering. Data fitting was carried out using Artemis code.[29] To account for structural disorder (i.e., Debye−Waller factors), fitting was performed on the basis of our MD simulations (section 3 in the Results). This new procedure will be thoroughly described in an upcoming paper. A total of five snapshots were used as model clusters for the calculation of the electronic parameters. In each snapshot, the Dy^{3+} cation was positioned at the center of a 6 Å water shell. The XAS electronic parameters were calculated using Feff82 code.[30] A total of eight backscattering paths were used in the fit for each snapshot, corresponding to the eight neighbors (CN = 8) of the Dy^{3+} cation. Only single scattering paths were considered, and backscattering from the hydrogen atoms was neglected. During the fit, the global amplitude reduction factor S_0^2, the threshold shift e_0, and the four structural parameters (d_{Rn}, u, v, w) were allowed to vary. For solution A (0.1 mol·L^{-1}), $S_0^2 = 1.00$ and $e_0 = 9.85$ eV. For solution G (3.0 mol·L^{-1}), $S_0^2 = 1.05$ and $e_0 = 9.97$ eV.

MD simulations were performed using AMBER6[31] and PMEMD[32] software programs with polarization. Water molecules are described using the POL3 model.[33] Dy^{3+} atomic polarizability was computed using GAUSSIAN 98[34] with a relativistic effective large-core potential (and associated basis set) developed in the Stuttgart and Dresden groups.[35] Lennard-Jones parameters for Dy^{3+} were then adjusted for good agreement with generally admitted experimental structural data for the first hydration sphere (eight H_2O molecules at 0.237 nm).[36−40] Exclusively nonbonded terms (electrostatic, Lennard-Jones, and polarization) were used to describe interactions between Dy^{3+} and surrounding molecules to allow water and chloride exchanges around the cation. Parameters for Cl^- anions were taken from the work of Smith et al. on NaCl solutions with potential including polarizability effects.[41] Molecular volumes have been computed using MSMS[42] with a 0.15 nm probe sphere (matching with one water molecule volume). This

TABLE 1: Molecular Dynamics Simulation Characteristics: Total Simulated Time (t), Number of Dy^{3+} Cations ($N(Dy^{3+})$), Number of Cl^- Anions ($N(Cl^-)$), and Number of H_2O Molecules Per Dy^{3+} Cation ($R(H_2O/Dy^{3+})$)

	sim(D1)	sim(D2)	sim(0.5)	sim(0.9)	sim(1.7)	sim(3.1)
t (ns)	2	2	4	2	2	4
$N(Dy^{3+})$	1	1	6	12	36	39
$N(Cl^-)$	0	3	18	36	108	117
$R(H_2O/Dy^{3+})$	1107	2138	121.5	60	33	18

procedure allows a description of volumes accessible to the solvent. For a given simulation, molecular volumes were computed for each snapshot, taken every 1 ps; the volumes shown in the Results represent an average of all the volumes issued from each snapshot. All studied systems were equilibrated for at least 100 ps by raising the temperature from 100 to 300 K. Periodic boundary conditions were used at constant pressure with a 1.2 nm cutoff, using Ewald summation (particle mesh Ewald algorithm built in AMBER). MD simulation analysis was performed using MDS[43] and VMD[44] procedures. Characteristics of the main simulations are reported in Table 1.

Theoretical Background

In this section, we shortly recall the theoretical aspects used in this work regarding the BIMSA.

The BIMSA theory is one of the derivatives of the mean spherical approximation (MSA).[45] As for the MSA, the BIMSA takes into account, at a microscopic scale, hard-core repulsion and Coulombic interaction. The main difference is that the BIMSA also considers a short-range potential, responsible for complex formation. In the present model, one cation and one anion can form a pair, a pair being defined as two ions of opposite charge being in contact and modeling a 1:1 stoichiometry complex. Furthermore, one central cation and two anions can form a trimer, defined as two anions in contact with a cation in a central position, modeling a 1:2 stoichiometry complex.

The effect of association is included in the computation of the MSA screening parameter Γ.[46] The resulting thermodynamic excess properties can be expressed in a simple way in terms of Γ when using the Wertheim formalism,[46] in which the thermodynamic association constants K_1° and K_2°, permit all associating mechanisms (Coulombic and covalent) to be taken into account. This formalism was shown to be successful for ionic solutions in both the hypernetted chain approximation and the MSA.[47]

In this work, we take into account the fact that the cation size and the permittivity are concentration dependent.[48] Let us underline that experimental data for the variation of the macroscopic solution permittivity with concentration are not expected to constitute relevant input information into the model. This is so because, while this quantity refers to electrostatic interactions between ions at large separations (a situation met at low salt concentration), the representation of the electrostatic energy of a solution at high concentration significantly involves short ionic separations.

Thus, the diameter of the cation σ_+ and the inverse of the relative permittivity of solution ϵ^{-1} were taken as linear functions of the salt concentration C_S:

$$\sigma_+ = \sigma_+^{(0)} + \sigma^{(1)}C_S \qquad (1)$$

$$\epsilon^{-1} = \epsilon_W^{-1}(1 + \alpha C_S) \qquad (2)$$

with ϵ_W the relative permittivity of pure solvent ($\epsilon_W = 78.3$ for water at 25 °C).

These equations introduce two adjustable parameters, $\sigma^{(1)}$ and α, that are characteristic of the electrolyte, while $\sigma_+^{(0)}$, the cation diameter at infinite dilution, is characteristic of the considered cation. It must have a common value for all salts (in the present work, perchlorate, chloride, and nitrate) containing the same cation (in the present work, dysprosium(III)). As in refs 16−18, 49, and 50 the anion diameter σ_- is kept constant, with values taken from previous work[49] and used for a wide variety of salts: 0.453 nm for ClO_4^-, 0.362 nm for Cl^-, and 0.340 nm for NO_3^-.

The BIMSA used in the present work, recently utilized for uranyl salts, includes expressions that can be found in ref 51 derived from ref 52.

The BIMSA solution requires the calculation of the proportion of ion pairs, trimers, and free ions deduced from the thermodynamic formation constants K_1° and K_2° related to the equilibria

$$Dy^{3+} + A^- \leftrightarrow DyA^{2+} (K_1^0) \qquad (3)$$

$$DyA^{2+} + A^- \leftrightarrow DyA_2^+ (K_2^0) \qquad (4)$$
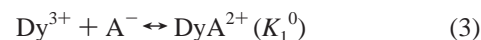
The solution of this BIMSA model was performed using a FORTRAN program, which can be run on a microcomputer. To optimize the different parameters, and minimize the difference between our calculated osmotic coefficient values and those existing in the literature,[3,4,7] a least-squares algorithm of the Marquardt type was used.

For comparison with experimental data, these quantities were converted from the McMillan−Mayer to the Lewis−Randall (LR, experimental) reference system[53] by using the procedure described in ref 49. The second classic transformation from molal scale to molar scale at the LR level was done. These transformations were conducted using dysprosium perchlorate, chloride, and nitrate high-accuracy ($\pm 1 \times 10^{-2}$ kg·m^{-3} for $DyCl_3$) solution density values of Spedding et al.[28,54,55]

The value of $\sigma_+^{(0)}$ was refined in a first step. As done in previous work,[49−51] $\sigma_+^{(0)}$ refinement was performed by fitting the perchlorate salt osmotic coefficient (dysprosium perchlorate in the present work). This procedure is justified by the fact that most perchlorate salts are the simplest systems to study because they are likely strong electrolytes (see the next section), so $K_1^\circ = K_2^\circ = 0$. In the second step, this value was used for fitting osmotic coefficients for aqueous dysprosium chloride and nitrate solutions.

Results

1. BIMSA Modeling. In this part, we fitted osmotic coefficient data for solutions of dysprosium perchlorate, chloride, and nitrate. Our selected data were raw values obtained by Spedding and Rard et al.[3,4,7] from isopiestic equilibrium measurements, for concentrations above 0.09 mol·kg^{-1} up to maximum concentrations comparable to those of previous work.[17] The numerous osmotic coefficient values of Spedding and Rard et al. are of high accuracy (typically 0.3%) and in good agreement with other measurements.[56]

Perchlorates are generally regarded as noncomplexing anions. This conclusion seems established for all lanthanide(III) perchlorate salts by various experimental methods. From UV−vis spectroscopy in aqueous medium at 25 °C, Silber et al. detected no neodymium(III) or erbium(III) perchlorate complexes despite the high perchlorate concentration of 3.0 M.[57] Also Silber[58] obtained the same results from ultrasonic absorption measurements on 0.2 M $Eu(ClO_4)_3$ at 25 °C. Johansson and Wakita,[59] from X-ray scattering measurements, found for La^{3+},

TABLE 2: BIMSA Parameter Values for Lanthanide Chloride, Nitrate, and Perchlorate

salt	max m^a	$\sigma_+^{(0)\,b}$	$10^3\sigma^{(1)\,c}$	$10^2\alpha^d$	$K_1^{\circ\,d}$	$K_2^{\circ\,d}$	AARD^e (%)
$Dy(ClO_4)_3$	1.9	0.951	−85.3	35.4	0	0	0.40
$DyCl_3$	2.4		−71.6	17.7	5.49	0.63	0.68
$DyCl_3^f$			−71.5	24.0	3.96	0	0.89
$Dy(NO_3)_3$	2.8		−65.3	28.8	2.20	0.41	0.88
$Dy(NO_3)_3^f$			−65.5	34.9	1.04	0	1.11

^{a} Given in $mol\cdot kg^{-1}$. ^{b} Value in nm. ^{c} In $nm\cdot mol^{-1}\cdot L$. ^{d} In $mol^{-1}\cdot L$. ^{e} AARD is the relative deviation for the calculated osmotic coefficients: AARD (%) = $(100/N)\sum_{k=1}^{N}|\Phi_{calcd}(k) - \Phi_{exptl}(k)|/\Phi_{exptl}(k)$, with N being the number of data points, Φ_{calcd} the calculated osmotic coefficient from the BIMSA, and Φ_{exptl} the experimental osmotic coefficient.[3,4,7] ^{f} Results obtained without taking 1:2 complex formation into account.

Tb^{3+}, and Er^{3+} selenate complexation but no indication of perchlorate complexation, even up to very high salt concentration ($[Er(ClO_4)_3]$ = 2.96 M, $[HClO_4]$ = 0.2 M). Breen and Horrocks[60] and Bünzli and Yersin[61] lifetime measurements on Eu salts suggested europium complexation by nitrate, but no evidence of complexation by perchlorate was detected.

Considering these observations, we assumed that Dy^{3+} does not form inner-sphere complexes with the perchlorate anion (i.e., $K_1^\circ = K_2^\circ = 0$). Therefore, a three-parameter fit ($\sigma_+^{(0)}$, $\sigma^{(1)}$, α) on the $Dy(ClO_4)_3$ experimental osmotic coefficient led to a hydrated Dy(III) diameter, $\sigma_+^{(0)}$, of 0.951 nm, and $\sigma^{(1)}$ and α values given in Table 2, with a very low AARD of 0.40%. As expected, these values are identical to those obtained from our previous BIMSA model without 1:2 complex formation.[17]

The hydrated cation radius at infinite dilution, $\sigma_+^{(0)}/2 = 0.475$ nm, can be compared to distances found in the literature for dysprosium perchlorate solutions. Yamaguchi et al.[37] from EXAFS measurements found a distance from Dy^{3+} to the oxygen of the first coordination sphere ($d(Dy-O_{(1)})$) equal to 0.237 ± 0.002 nm. This value is in good agreement with distances found from neutron diffraction studies. Cossy et al.[62] found $d(Dy-O_{(1)}) = 0.239 \pm 0.002$ and 0.240 ± 0.002 nm, in agreement with Yamaguchi et al.[63] These measurements, conducted in D_2O solvent, also provided values for $d(Dy-D_{(1)})$, the distance between Dy^{3+} and a deuterium atom of the first D_2O coordination sphere: Cossy et al.[62] found a $d(Dy-D_{(1)})$ value of 0.303 ± 0.002 nm, which is in reasonable agreement with the Yamaguchi et al.[63] $d(Dy-D_{(1)})$ value of 0.308 ± 0.003 nm. These distances, noticeably lower than our $\sigma_+^{(0)}/2$ value, show that the BIMSA hydrated cation diameter accounts for water molecules beyond the first layer, in agreement with the generally admitted picture that lanthanide(III) cations are surrounded by more than one hydration layer.[26] EXAFS and neutron scattering methods also provided such distances (between Dy^{3+} and water molecules of the first hydration sphere) in the case of $DyCl_3$ or $Dy(NO_3)_3$ solutions.[39,40] For the latter salts, within experimental uncertainties, no noticeable deviation from the values obtained for $Dy(ClO_4)_3$ solutions were observed: for a binary $DyCl_3$ solution, Annis et al.[39] obtained a distance $d(Dy-O_{(1)})$ of 0.2370 ± 0.0003 nm.

In contrast, techniques providing structural information on the second hydration layer are scarce. Such values can be calculated using X-ray diffraction measurements.[19,36,59,64] For a system similar to a $Dy(ClO_4)_3$ aqueous solution (Z = 66), namely, $Tb(ClO_4)_3(Z = 65)/HClO_4$ within a Tb:H ratio value of 3.12, Johansson and Wakita[59] reported a distance $d(Tb-O_{(1)})$ = 0.2400 ± 0.0005 nm and a distance from Tb^{3+} to the oxygen of the second coordination sphere, $d(Tb-O_{(2)})$, equal to 0.460 nm. The latter is close to our value for $\sigma_+^{(0)}/2$ (0.475 nm) in the case of dysprosium perchlorate. However, the identification
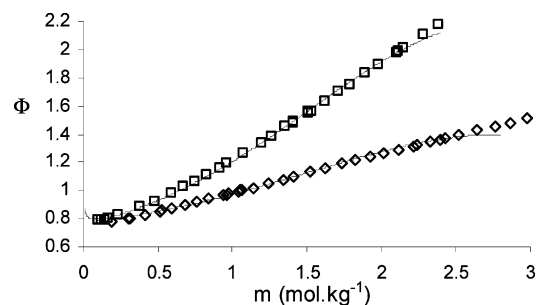
Figure 1. Osmotic coefficient calculated from the BIMSA theory by taking into account 1:1 and 1:2 complex formation (solid line) and experimental $DyCl_3$ (□) and $Dy(NO_3)_3$ (◇).[3,7]

of our hydrated lanthanide(III) diameter with $d(Ln-O_{(2)})$ is not clear.

Finally, the $\sigma_+^{(0)}$ value of 0.951 nm is in excellent agreement with, to our knowledge, the only value in the literature for the hydrated Dy^{3+} diameter, 0.950 nm proposed by David and Fourest[65] from three transport properties (diffusion, mobility, and conductivity) at zero ionic strength.

Next, osmotic coefficients for dysprosium nitrate and chloride were fitted using the BIMSA model, with the $\sigma_+^{(0)}$ value obtained in the case of $Dy(ClO_4)_3$ (these salts having the Dy^{3+} cation in common[49]), which led to the adjustment of the four parameters $\sigma^{(1)}$, α, K_1^0, and K_2^0. Table 2 compares the present results with those of the previous model in which the 1:2 complex formation was not taken into account. Figure 1 compares the experimental and calculated osmotic coefficients for the $DyCl_3$ and $Dy(NO_3)_3$ salts.

We can see in Table 2 that the quality of fit is significantly improved when 1:2 complex formation is taken into account. The average relative deviation is decreased by 0.2% in the chosen concentration range. Actually, despite the fact that our calculated K_2° values are low, the proportion of the 1:2 complex for concentrated solutions is high enough to modify the value of the osmotic coefficient. Then the $\sigma_+^{(0)}$ value of 0.951 nm, which does not allow a very good representation of nitrate dysprosium salt osmotic coefficients when only 1:1 complex formation is taken into account,[17] provides acceptable results with reasonable discrepancies when the second association is also taken into account (Figure 1). However, at high concentration, a systematic deviation appears for $DyCl_3$ and $Dy(NO_3)_3$, the osmotic coefficient being underestimated.

Lanthanide(III) complexation by nitrate and chloride has been widely studied with different methods. As examples, association constants were calculated from titration,[66] microcalorimetry,[67] NMR,[68] UV−vis spectroscopy,[69] luminescence excitation spectroscopy,[60] solubility measurements,[70] Raman spectroscopy,[71] solvent extraction,[21,72] and ion exchange.[24] Many authors showed that lanthanide(III) chlorides or nitrates form 1:1 complexes and also 1:2 complexes.[19−25] This may explain the noticeable improvement made when we consider 1:1 and 1:2 association constants in the BIMSA model (Table 2). Besides, the values issued from our fit on dysprosium chloride and nitrate are in agreement with the general observation that the second complex formation is weaker than the 1:1 complex formation ($K_2 < K_1$).[20,21,23−25] Thus, the second association was sometimes neglected, especially when work was being done on dilute solutions.[73] Unfortunately, comparing our thermodynamic constants K_1° and K_2° with the constants reported in the literature is not straightforward because the latter are essentially apparent constants at high ionic strength.

Regarding 1:1 complexes, Millero[74] and Wood[73] obtained a selection of existing lanthanide nitrate and chloride data and

TABLE 3: Thermodynamic 1:1 Complex Formation Constants for Dysprosium(III) Nitrate and Chloride

salt	Wood[70,73]	Millero[74]	Majdan et al.[72]	Bonal et al.[67]	Luo et al.[66]	BIMSA[a]
$DyCl_3$	2.04	1.86			4.47	5.49
$Dy(NO_3)_3$		1.41	21	1.2		2.20

[a] This work (results from BIMSA theory with 1:1 and 1:2 complex formation).

extrapolated apparent constants to thermodynamic constants using Pitzer parameters and an extended Debye−Hückel equation. Majdan and Sodowski[72] and Bonal et al.[67] proposed thermodynamic constants for dysprosium nitrate. Luo and Byrne[66] extrapolated lanthanide chloride apparent constants to zero ionic strength. Table 3 shows the 1:1 thermodynamic constants for dysprosium nitrate and chloride, proposed by the different authors, in comparison to our calculated values of the BIMSA thermodynamic constant. Our calculated 1:1 $DyCl^{2+}$ or $DyNO_3^{2+}$ thermodynamic formation constants are in reasonable agreement with most of the values proposed in the literature. More precisely, our constants are very close to Luo and Byrne[66] data for dysprosium chloride and very close to Millero[74] extrapolated data from Pitzer equations in the case of dysprosium nitrate. The value of Majdan and Sadowski[72] for dysprosium nitrate (using liquid−liquid extraction) seems overestimated, considering Millero compilation[74] and Bonal et al. data.[67]

Literature values for $K_2°$ are scarce. Haas et al.[75] proposed the value $K_2° = 0.85$ for $DyCl_2^+$, taken from the 1:1 thermodynamic constant calculated by Millero[74] and adjusted using an empirical equation. This value is in good agreement with our calculated value, $K_2° = 0.63$.

Note that 1:3 complex formation is likely to be low as shown by Silber and Strozier using UV−vis spectroscopy in aqueous solution.[69]

Regarding our $\sigma^{(1)}$ value, as in previous work, the expected condition $\sigma^{(1)} < 0$ is satisfied. Moreover, $\sigma^{(1)}$ increases in absolute value with the size of the anion (Table 2), which conveys the idea that the bigger the anion, the faster the hydration number of the cation decreases.[49] In practice, structural modification of the first and higher hydration layers with concentration has seldom been studied: generally, studies were conducted on ternary systems (such as LnX₃/HX/H₂O), for only one or two different concentrations. Therefore $\sigma^{(1)}$ values are difficult to correlate to literature values. The expected condition $\alpha > 0$ is also satisfied.

The results of this section lead to the following conclusions: All BIMSA parameters seem to have plausible values. They allow a good representation of osmotic coefficients for perchlorate, chloride, and nitrate salts. The complex formation constants are in general in good agreement with values "more directly" obtained from experiment.

2. Spectroscopic Measurements. Spectroscopic measurements were performed to study the first coordination sphere of Dy^{3+} with concentration from 0.1 to 3.0 $mol \cdot L^{-1}$.

It is well-known that modification of the first coordination shell of a given ion can change the features of UV−vis−near-IR spectra (absorption wavelength and molar extinction coefficient). Therefore, since Dy^{3+} absorbs in the UV−vis−near-IR region, its salts are adequate for spectrophotometric investigation on the modifications of the first coordination sphere.

The $DyCl_3$ spectral analysis at various concentrations (solutions A−G, from 0.1 to 3.0 $mol \cdot L^{-1}$) shows that the Beer−Lambert law is verified for all important absorption bands. Furthermore, the band properties (maximum absorption wave-

length, fwhm) are not modified (Table S1 in the Supporting Information). For clarity only the spectrum of the $DyCl_3$ 1.5 $mol \cdot L^{-1}$ solution (D) is represented in Figure 2. It shows the characteristic absorption bands of Dy^{3+}, including the signals in the 300−500 nm region and four absorption signals between 700 and 1200 nm.[76] The hypersensitive absorption signal at 1290 nm was not studied in our experimental conditions. Comparison of $DyCl_3$ spectra with $Dy(ClO_4)_3$ in $HClO_4$ spectra was made (solutions X−Z, from 0.64 to 2.56 $mol \cdot L^{-1}$) (Figure 2). No difference could be observed: $DyCl_3$ and $Dy(ClO_4)_3$ absorption peak wavelengths and molar extinction coefficients are identical. The similarity of the spectra indicates that chloride ions do not form inner-sphere complexes with dysprosium(III). To confirm these results, comparison was made with the reflection spectrum of the $DyCl_3 \cdot 6H_2O$ solid (S). Actually, it was shown in ref 27 that, in the solid $DyCl_3 \cdot 6H_2O$ compound, two chloride ions are part of the dysprosium(III) first coordination shell. The solid spectrum, compared to dysprosium(III) chloride or perchlorate solution spectra, shows that the chloride ions in the dysprosium-(III) first coordination shell noticeably modify the wavelengths of the absorption peaks, particularly in the 740−850 nm region (Figure 2).

The literature shows that modification of the dysprosium-(III) environment may dramatically modify its fluorescence properties.[77] Therefore, we chose to compare the fluorescence spectra and lifetimes of our solutions (solutions A−G and X−Z). In the particular case of Dy^{3+}, transition from the $^4F_{9/2}$ level to the $^6H_{15/2}$ and $^6H_{13/2}$ levels leads to the emission wavelengths at 483 and 580 nm, respectively. It should be noted that Dy^{3+} hypersensitive transition between $^6F_{11/2}$ to $^6H_{15/2}$ levels is difficult to observe since it is located in the infrared region.

Figure 3 shows the Dy^{3+} fluorescence spectrum of $DyCl_3$ at 2.5 $mol \cdot L^{-1}$ (solution F) and $Dy(ClO_4)_3$ at 1.28 $mol \cdot L^{-1}$ (solution Y). The most important feature is the absence of modification of the spectrum in terms of wavelength shift or splitting between the chloride salt and the perchlorate salt, indicating a similar environment of the Dy^{3+} cation. The same observation was made when the $DyCl_3$ (and $Dy(ClO_4)_3$) samples at other concentrations were compared. Moreover, Figure S1 in the Supporting Information shows the variation of the Dy fluorescence intensity as a function of the binary $DyCl_3$ concentration from 0.1 to 3.0 $mol \cdot L^{-1}$. The fluorescence signal varies linearly with concentration up to 1.5 $mol \cdot L^{-1}$. Above this concentration, self-quenching occurs, leading to a decrease in fluorescence.

The absence of modification of the spectral observations are further confirmed by analyzing the fluorescence lifetime for $DyCl_3$ solutions (from solution A to solution G). Hence, Table S2 in the Supporting Information presents the $^4F_{9/2}$ dysprosium lifetimes (τ) for $DyCl_3$ solutions, measured at 483 and 580 nm. The lifetime does not change significantly with concentration and is equal to 2.7 ± 0.4 μs, compatible with eight water molecules left in the first coordination sphere using the equation $n(H_2O) = 0.024/\tau - 1.3$ (τ in milliseconds).[78]

The fitted EXAFS spectra of solutions A and G are presented in Figure 4. Fits are of very good quality. In particular, the well-adjusted amplitude of the fitted curve at large k reflects the good estimation of disorder with molecular dynamics snapshots obtained from our calculations (section 3). The best fitted Dy−O distances obtained from EXAFS data (Figure 4) confirm the absence of modification of the cation first hydration shell from a dilute system, up to very high concentration. For diluted solution A (0.1 $mol \cdot L^{-1}$), eight water molecules (CN fixed; see

Lanthanide and Actinide Solution Thermodynamics

J. Phys. Chem. A, Vol. 110, No. 41, 2006 **11775**
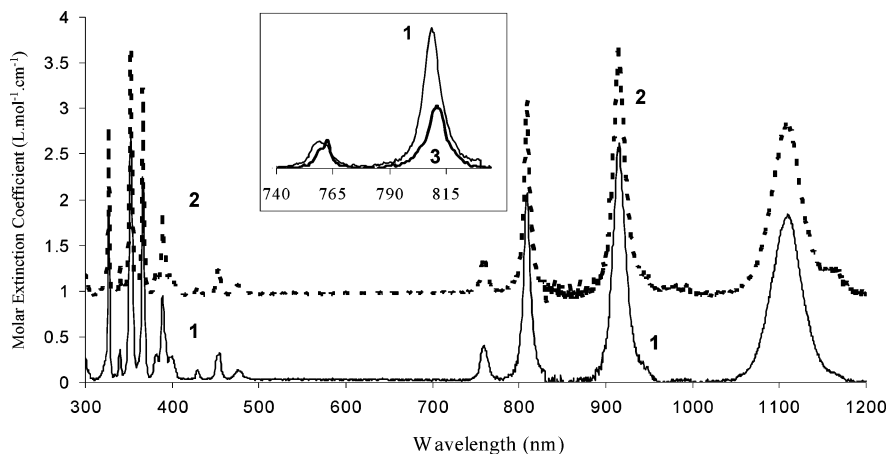
Figure 2. UV−vis−near-infrared spectra of (1) a normalized DyCl$_3$ solution (1.5 mol·L^{-1}), (2) a normalized Dy(ClO$_4$)$_3$ solution (1.28 mol·L^{-1}) with HClO$_4$, and (3) DyCl$_3$·6H$_2$O solid compound. Assignments of the bands can be found in ref 76.
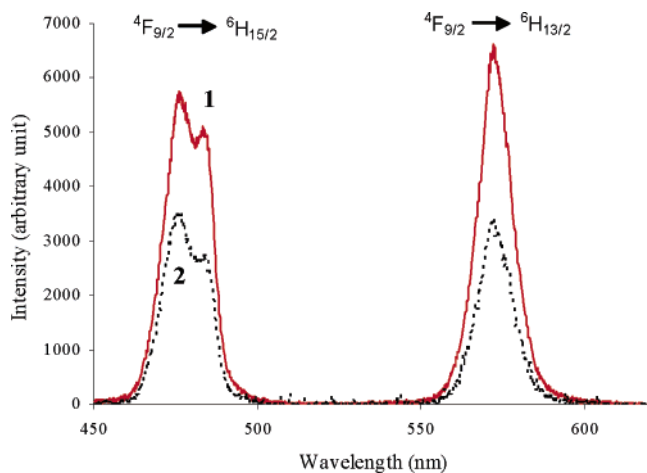
Figure 3. Fluorescence spectrum of (1) DyCl$_3$ (2.5 mol·L^{-1}) and (2) Dy(ClO$_4$)$_3$−HClO$_4$ ([Dy(ClO$_4$)$_3$] = 1.28 mol·L^{-1}).
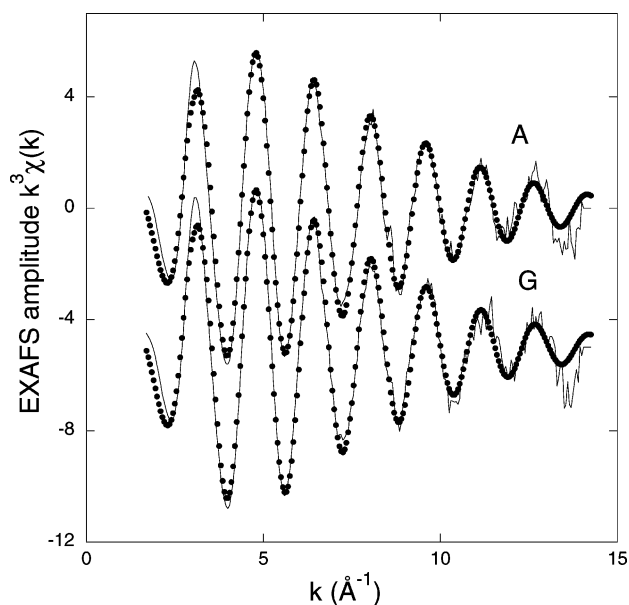
Figure 4. Experimental and adjusted EXAFS spectra at the Dy L$_{III}$ edge of solutions A ([DyCl$_3$] = 0.1 mol·L^{-1}) and G ([DyCl$_3$] = 3.0 mol·L^{-1}): (−) experimental spectrum, (●) fitted spectrum.

the Experimental Section) are located at an average distance of 0.238 nm. This feature is in remarkable agreement with the literature data listed previously (see BIMSA Modeling). For the

more concentrated solution G (3.0 mol·L^{-1}), similar structural parameters have been obtained: eight water molecules (CN fixed) at 0.238 nm. The assumption of fixing the same coordination number for both solutions is validated by the similar values of the global amplitude factor S_0^2 in the spectra of solutions A ($S_0^2 = 1.00$) and G ($S_0^2 = 1.05$). For both solutions, the absence of Cl$^-$ ions in the first coordination sphere, as observed by absorption or fluorescence spectroscopy, is confirmed.

The close similarity between DyCl$_3$ and Dy(ClO$_4$)$_3$ solution absorption or fluorescence spectra, combined with EXAFS results, indicate the absence of inner-sphere dysprosium(III) chloride complexes up to 3.0 mol·L^{-1} and seem also to show that the coordination number and inner-sphere distances are unchanged when the concentration becomes higher.

3. Molecular Dynamics Simulations. MD simulations were performed for various concentrations of DyCl$_3$ salt in water ranging from diluted to 3.1 mol·kg^{-1} solution. The simulation method was first validated by checking that solution densities matched experimental ones (Table S3 in the Supporting Information). The deviation between the two sets of values did not exceed 5%.

First, simulations for diluted solution were performed for different starting geometries, because the association or dissociation process of the Cl$^-$ anion in the vicinity of Dy^{3+} may occur at time scales longer than those easily reachable (some nanoseconds) in MD simulations. These simulations were built in all cases by taking one Dy^{3+} cation in a water box: without Cl$^-$ ions (sim(D1)), with three Cl$^-$ ions in the second coordination sphere of Dy^{3+} (sim(D2)), with three Cl$^-$ ions in the first coordination sphere of (i.e., associated with) Dy^{3+} (sim(D3)), or three Cl$^-$ ions outside these regions (i.e., nonassociated with Dy^{3+}) (sim(D4)).

Simulation sim(D1) allows one to describe the hydration of an isolated Dy^{3+} ion. The radial distribution function (RDF) centered on Dy^{3+}, hereafter denoted by $g_{Dy,Cl}$, shows (see Table 4) that the cation is surrounded by 8 water molecules at 0.237 nm and 18 water molecules at 0.460 nm in its first and second coordination spheres, respectively (Figure 5, left). Integration of the hydrogen atom RDF yields 16 atoms at a distance of 0.303 nm from Dy^{3+}, in agreement with neutron diffraction experiments.[62] The distance from Dy^{3+} ($Z = 66$) to the second sphere is close to an experimental value for Tb^{3+} ($Z = 65$) in perchlorate media,[59] d(Tb−O$_{(2)}$) = 0.456 nm.

Simulation sim(D2) (starting with three chloride anions located in the Dy^{3+} second coordination sphere) shows a quasi total dissociation of the anions during the simulation time (Fig-

11776 *J. Phys. Chem. A, Vol. 110, No. 41, 2006*

Ruas et al.

TABLE 4: Oxygen and Chloride Dy^{3+}-Centered RDF First Peak Characteristics

	sim(D1)	sim(D2)	sim(0.5)	sim(0.9)	sim(1.7)	sim(3.1)
$d(Dy-O_{(1)})^a$ (nm)	0.237	0.237	0.237	0.237	0.237	0.237
$n_{Dy}(O_{(1)})^b$	8	8	8	8	8	8
$d(Dy-O_{(2)})^a$ (nm)	0.46	0.46	0.46	0.46	0.46	0.46
$n_{Dy}(O_{(2)})^c$	18	17.5	17.5	17	15	10
$d(Dy-Cl)^a$ (nm)		0.52	0.52	0.52	0.52	0.52
$n_{Dy}(Cl)^d$		0.5	0.5	1.1	2.7	6.3

^{a} RDF peak maximum position. ^{b} Number of oxygens in the Dy^{3+} first coordination sphere. ^{c} Number of oxygens in the Dy^{3+} second coordination sphere. ^{d} Number of chlorides in the Dy^{3+} second coordination sphere.
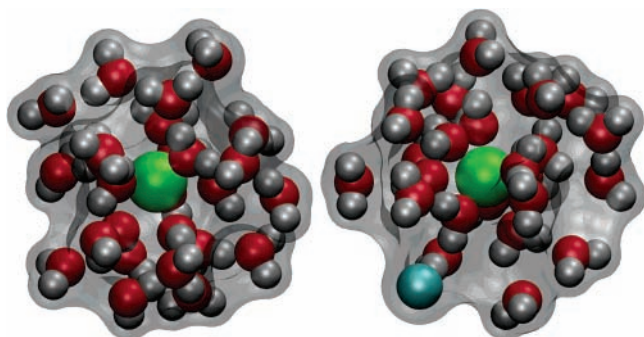
Figure 5. Snapshots from MD simulation of dilute solutions of [Dy^{3+}(H$_2$O)$_n$] (left, sim(D1)) and [Dy^{3+}(H$_2$O)$_n$(Cl$^-$)$_m$] (right, sim(D2)) clusters: Dy^{3+} (green), Cl$^-$ (blue), and water molecules in the first two solvation shells.

TABLE 5: Average Volumes (nm³) and Corresponding Diameters (nm) for [Dy^{3+}(H$_2$O)$_n$(Cl$^-$)$_m$] and [Dy^{3+}(H$_2$O)$_n$] Clusters

	Dy^{3+}(H$_2$O)$_n$(Cl$^-$)$_m$		Dy^{3+}(H$_2$O)$_n$	
simulation	volume	diameter	volume	diameter
sim(D1)			0.617 ± 0.04	1.056 ± 0.02
sim(D2)	0.619 ± 0.04	1.057 ± 0.02	0.616 ± 0.04	1.055 ± 0.02
sim(0.5)	0.624 ± 0.04	1.060 ± 0.02	0.609 ± 0.04	1.051 ± 0.03
sim(0.9)	0.628 ± 0.04	1.062 ± 0.02	0.581 ± 0.05	1.034 ± 0.03
sim(1.7)	0.642 ± 0.04	1.070 ± 0.02	0.559 ± 0.05	1.021 ± 0.03
sim(3.1)	0.658 ± 0.04	1.078 ± 0.02	0.424 ± 0.06	0.930 ± 0.04

ure 5 and Figure S2 in the Supporting Information). Integration of the RDF, $g_{Dy,Cl}$, indicates an average of 0.5 Cl$^-$ anion at 0.52 nm from the cation. Analyses of Dy^{3+}−Cl$^-$ distances show that Cl$^-$ ions do not remain in the second coordination sphere but exchange with the bulk. As in sim(D1), the first hydration sphere of Dy^{3+} is still filled with 8 water molecules (O$_{(1)}$ at 0.237 nm from Dy^{3+}), while there are 17 or 18 water molecules in the second sphere. Second-sphere distances are not modified ($d(Dy-O_{(2)}) = 0.46$ nm) when a chloride ion enters the cation second coordination sphere. sim(D3) and sim(D4) do not lead to an association of chloride ions with the cation neither in the first nor in the second coordination sphere, resulting in a Dy^{3+} hydration structure identical to that of sim(D1), i.e., without chloride ions.

Two clusters were considered for volume calculations. The first cluster, [Dy^{3+}(H$_2$O)$_n$(Cl$^-$)$_m$], was composed of one Dy^{3+} ion with its first two coordination spheres comprising water molecules and Cl$^-$ ions, at less than 0.53 and 0.58 nm from Dy^{3+}, respectively. The second cluster was [Dy^{3+}(H$_2$O)$_n$]. The volume accessible to water molecules (VAWM) was computed for these two clusters. The latter were approximated by spheres of the same volume, and the corresponding diameters were determined for comparison with the BIMSA σ_+ value. The results are reported in Table 5. For the simulations of diluted
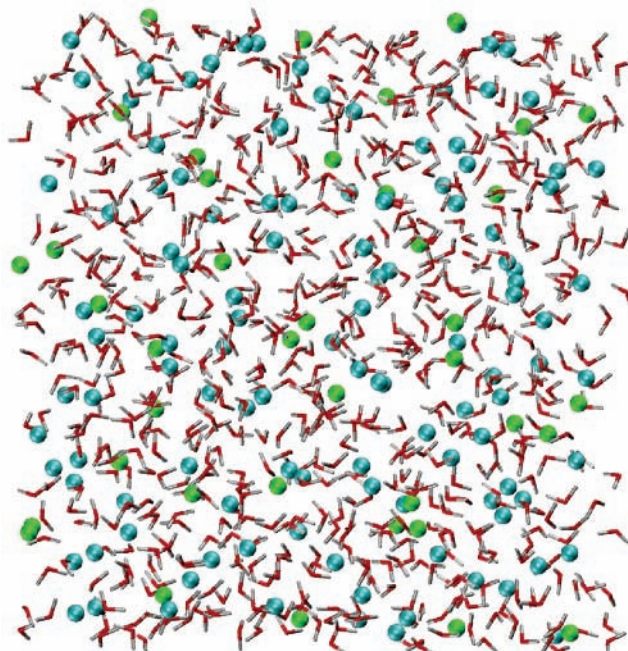
Figure 6. Simulation of a 3.1 mol·kg^{-1} DyCl$_3$ solution. Snapshot of the simulated box: Dy^{3+} (green) with Cl$^-$ (blue).

solutions, sim(D1) and sim(D2), the presence of Cl$^-$ ion in the Dy^{3+} second coordination sphere does not drastically change the cluster volumes. The corresponding higher diameter value obtained here (about 1.06 nm) is rather satisfactory as compared to the BIMSA $\sigma_+^{(0)}$ value of 0.95 nm, in view of the equivocal nature of molecular volume calculations. Despite this feature, this method of calculating the MD diameter value is adopted below for comparison with the BIMSA σ_+ value.

A 0.5 mol·kg^{-1} solution was simulated (sim(0.5)), starting with three Cl$^-$ ions associated with Dy^{3+} within the first coordination sphere. For this simulation, there was no Cl$^-$ ion remaining in the first coordination sphere of Dy^{3+} after 1 ns. The first coordination sphere remained unchanged with eight water molecules at 0.237 nm for the subsequent 3 ns. In its second coordination sphere, each Dy^{3+} was then surrounded by 18 water molecules, by 17 H$_2$O molecules and 1 Cl$^-$ ion, or sometimes by 16 H$_2$O molecules and 2 Cl$^-$ ions. As in the previous simulation, sim(D2), Cl$^-$ ions exchange between the bulk and cation neighborhood during the MD simulation, resulting in an average of 0.5 Cl$^-$ ion in each Dy^{3+} second coordination sphere (at 0.52 nm, Table 4).

MD simulations were performed for 0.9, 1.7, and 3.1 mol·kg^{-1} DyCl$_3$ solutions, starting with one Cl$^-$ ion in the second sphere (sim(0.9), sim(1.7), and sim(3.1)). Even for these more concentrated solutions, there was no Cl$^-$ ion directly bonding to Dy^{3+} along the MD simulations, maintaining in all cases the intactness of the cation first coordination sphere, with eight water molecules (O$_{(1)}$ at 0.237 nm), as for diluted solutions (Table 4). This finding is in agreement with our present experimental results (UV−vis, TRLFS, and EXAFS). When the solution concentration was increased to 3.1 mol·kg^{-1}, no modification of Dy^{3+} distances to water or chloride atoms in the second coordination sphere was observed. On the other hand, a high salt concentration clearly favors the presence of chloride ions in the cation second sphere. The average number of water molecules in the second sphere decreases from 17.5 to 10 and the average number of Cl$^-$ ions increases from 0.5 to 6.3 when the concentration is increased from 0.5 to 3.1 mol·kg^{-1} (Figures 7 and 8).

Lanthanide and Actinide Solution Thermodynamics

J. Phys. Chem. A, Vol. 110, No. 41, 2006 **11777**
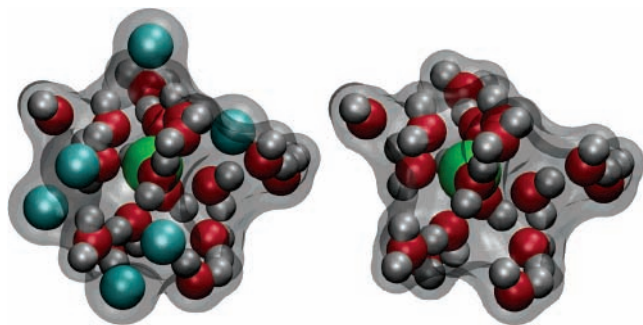
Figure 7. DyCl$_3$ solution simulation at 3.1 mol·kg^{-1}. Snapshots for [Dy^{3+}(H$_2$O)$_n$] (right) and [Dy^{3+}(H$_2$O)$_n$(Cl$^-$)$_m$] (left) clusters: Dy^{3+} (green), Cl$^-$ (blue), and the first two solvation shell water molecules.
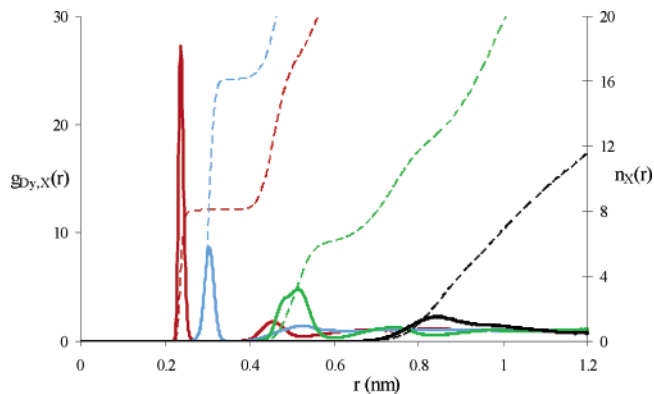
Figure 8. Simulation of a 3.1 mol·kg^{-1} DyCl$_3$ solution (simulation sim(3.1)): RDF of X in the neighborhood of Dy^{3+} ($g_{Dy,X}$, full line), integrated RDF of X at distance r from Dy^{3+} ($n_X(r)$, dotted line). X = water oxygen (red), water hydrogen (blue), Cl$^-$ (green), and Dy^{3+} (black).

TABLE 6: Cl$^-$-Centered RDF First Peak Characteristics

	sim(D2)	sim(0.5)	sim(0.9)	sim(1.7)	sim(3.1)
d(Cl−H$_{(1)}$)^a (nm)	0.229	0.230	0.226	0.228	0.225
d(Cl−O$_{(1)}$)^a (nm)	0.325	0.320	0.322	0.321	0.319
n_{Cl}(H$_{(1)}$)^b	6.8	6.8	6.7	6.7	6.3

^{a} RDF peak maximum position. ^{b} Number of hydrogens in the Cl$^-$ first coordination sphere.

For all simulated solutions, chloride ions are coordinated by six or seven water molecules (Table 6). Note that the distance d(Cl−H$_{(1)}$), separating water in the first coordination sphere from Cl$^-$, ranged from 0.225 to 0.230 nm, which is in good agreement with experimental neutron diffraction results (from 0.222 to 0.229 nm) obtained for various chloride salts.[79]

The VAWM and the corresponding diameters were computed for [Dy^{3+}(H$_2$O)$_n$(Cl$^-$)$_m$] and [Dy^{3+}(H$_2$O)$_n$] clusters from the last simulations (sim(0.5), sim(0.9), sim(1.7) and sim(3.1)). The results reported in Table 5 and Figure 9 show, as expected, that the average diameter of the [Dy^{3+}(H$_2$O)$_n$(Cl$^-$)$_m$] cluster increases with concentration from 1.057 (sim(D2)) to 1.078 nm (3.1 mol·kg^{-1} solution), due to the addition of Cl$^-$ ions in the Dy^{3+} second coordination sphere for highly concentrated solutions. For the same reason, clusters without chloride anions ([Dy^{3+}(H$_2$O)$_n$]) decrease in diameter by 0.125 nm between a dilute solution and a 3.1 mol·kg^{-1} solution. Since the distance between Dy^{3+} and the first- or second-sphere water oxygen atom does not vary when the concentration is increased, the decrease of the "hydrated cation" diameter results only from the increase of the number of Cl$^-$ ions in the second coordination sphere of Dy^{3+}.
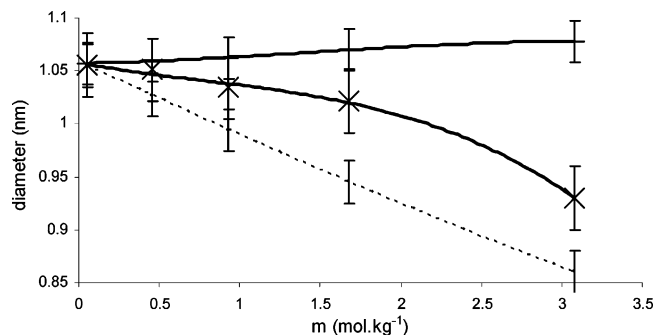
Figure 9. Comparison of size variations with concentration: [Dy^{3+}(H$_2$O)$_n$(Cl$^-$)$_m$] cluster diameter (from MD simulations, full line), [Dy^{3+}(H$_2$O)$_n$] cluster diameter (from MD simulations, solid line with bisecting times signs), and BIMSA hydrated cation diameter σ_+ (dotted line). The diameters are assumed to have equal values at 0.05 mol·kg^{-1}.

Discussion

The influence of the concentration of a binary lanthanide salt solution on the structure of the lanthanide ion in aqueous solution has been scarcely studied. In most cases, in the literature, the influence of concentration has been studied for mixtures in which the presence of a second cation (typically H$^+$, Li$^+$, or Na$^+$) was expected to disturb the lanthanide salt behavior.[80] Some studies were done on binary lanthanide salt solutions,[36,39] but assessment of the influence of the binary lanthanide(III) salt concentration on the structural properties of the cation and anion was in general difficult because the binary was not studied at different concentrations. By studying seven DyCl$_3$ binaries, from relatively dilute (0.1 mol·kg^{-1}) up to high concentration (3.36 mol·kg^{-1}) using different methods, we were able to assess accurately the structural modifications in dysprosium chloride solutions.

Regarding the cation first hydration shell, whatever the method, no structural change was noticed in the range of dilute to highly concentrated DyCl$_3$ solutions. Distances were found unchanged according to MD calculations and EXAFS measurements. The different studies showed that the number of water molecules in the first hydration sphere (generally admitted to be eight for dysprosium(III)) is not modified.

They showed also the absence of Cl$^-$ ions in the Dy^{3+} first coordination shell. This observation may seem surprising in view of the total number of water molecules available per cation at high concentration: for example, 18 at a concentration of 3.1 mol·kg^{-1} (Table 1 and Figure 6). In that case, from a stoichiometric point of view, Dy^{3+} being bonded to 8 water molecules, this leaves only 10 water molecules for the Dy^{3+} second sphere, Cl$^-$ coordination, and bulk. Considering the global 1:3 stoichiometry of the salt, we would expect the presence of chloride ions in the first coordination shell of the dysprosium(III) cation.[36] However, all the methods agree against this assertion: even at high concentration, chloride and dysprosium ions are separated by water molecules.

Also, just from the stoichiometry, one can say that neighboring cations dynamically share their second sphere of water molecules and also that a high proportion of chlorides constitute a solvent-separated ion pair with dysprosium(III), shared between two neighboring Dy^{3+} cations. This was observed during MD simulations (Figures 7 and 8).

Besides, molecular dynamics, despite giving a "dynamic" description of the solution, very different from the "static", time-averaged description from the BIMSA, provides structural information compatible with the BIMSA theory. Hence, MD calculations allowed us an interpretation of the BIMSA param-

eters $\sigma_+^{(0)}$ and $\sigma^{(1)}$ (respectively the hydrated cation diameter and parameter of the diameter decrease with concentration) that was not immediate from other methods. The distance $d(\text{Dy}-\text{O}_{(1)})$ and also the distance $d(\text{Dy}-\text{O}_{(2)})$ not changing significantly with concentration, the BIMSA hydrated cation diameter σ_+, which is expected to decrease, cannot be correlated to cation—water molecule distances. On the other hand, the hydrated cation diameter σ_+ could be identified as the diameter of a sphere which has the same volume as the cation plus the water molecules constituting its first and second hydration layers (Figure 9; for better comparison, the value for $\sigma_+^{(0)}$ given in Table 2 has been modified to obtain similar distances at low concentration).

From the agreement between different existing approaches such as MD and the BIMSA, we expect to be able to provide microscopic data for using in the future the lowest number of parameters possible or for improving the latter theory.

At infinite dilution, the volume of a cluster including a given lanthanide(III) or actinide(III) and water molecules of its first and second hydration layers provided by MD may be correlated to the BIMSA parameter $\sigma_+^{(0)}$. $\sigma_+^{(0)}$ deduced from transport properties using the Stokes equation to calculate hydrated lanthanide(III) and actinide(III) diameters[65] should also be considered as an alternative to provide an input parameter within the BIMSA.

Our fitted thermodynamic complex formation constants $K_1°$ and $K_2°$ are very close to thermodynamic constants that could be found in the literature. Therefore, in future work on the actinide(III), reliable literature values could be taken as input parameters. This approach has already been used successfully for uranyl(VI) salts.[51]

Regarding the hydrated cation size decrease with concentration (parameter $\sigma^{(1)}$), in the special case of dysprosium chloride, according to our MD calculations, a linear decrease of σ_+ with concentration is expected to be less realistic than a polynomial decrease (Figure 9). Also, according to MD, the hypothesis consisting of neglecting the anion coordination might need reviewing. Finally, despite the fact that correlation should be less straightforward, an analysis of the dynamic behavior of the water molecules might give some indication as to the permittivity variation with concentration (parameter α) and help us to improve the current model regarding this aspect. Then we hope to use the MD—BIMSA theory coupling to noticeably improve the potential predictivity of the BIMSA.

To gain more quantitative information from the molecular dynamics simulations, for use as input into the BIMSA model, some aspects would need deeper investigations. For example, to give accurate time-averaged properties or parameter values, our MD calculations need to be run for a time longer than a few nanoseconds. Finally, if we plan to use MD as a reliable tool for the BIMSA predictive application of the actinides(III), some aspects other than polarization should be considered, such as charge-transfer effects (as mentioned by Clavagera et al.[81]) that are negligible in the case of lanthanide(III) ions.

Conclusion

The BIMSA model, including chemical association combined with a Bjerrum-like exponential closure, has been shown to allow good representation of the thermodynamic properties of dysprosium perchlorate and of the associating electrolytes dysprosium nitrate and chloride, up to high concentration, by using a reasonably low number of parameters (three in the case of dysprosium perchlorate and four in the case of dysprosium nitrate and chloride), by following a simple and straightforward

protocol. By taking into account 1:1 and 1:2 complex formation, the deviation of the calculated BIMSA osmotic coefficients from the experimental ones has been noticeably decreased.

The use of UV—vis spectroscopy, TRLFS, and EXAFS on binary DyCl_3 solutions showed that the first coordination sphere of the lanthanide(III) cation is not modified in the concentration range $0-3.36$ mol·kg^{-1}.

MD calculations were done on the same DyCl_3 binary system from dilute to 3.1 mol·kg^{-1} as an attempt to better correlate the BIMSA parameters with microscopic features, and to improve the model. A first physical interpretation of the diameter of the hydrated cation was proposed in terms of the volume of the lanthanide(III) and its first two hydration layers.

The MD calculations, combined with analysis of literature data (especially in the case of thermodynamic complex-formation constants), showed that our BIMSA parameters, optimized on a macroscopic property of the solution (the osmotic coefficient variation with concentration), had, from a microscopic point of view, reasonable adjusted values.

This observation suggests that, in the future, the BIMSA theory could be used in a predictive way, by means of input data provided by other methods, thus reducing the number of model parameters to be adjusted. Thus, the BIMSA may be regarded as a valuable tool for predicting thermodynamic properties.

In future work, we hope to use MD calculations on other binary salt solutions to investigate more in depth possibilities of better taking into account the hydrated cation structure, permittivity modification with concentration, and coordination structure of the anions. We also hope, due to the successful results obtained for the lanthanide(III) solutions, to be able to predict the thermodynamic properties of actinide(III) salts, which are difficult to study experimentally because of their high radioactivity.

Supporting Information Available: Complete refs 31a and 34, Figures S1 and S2, and Tables S1—S3. This material is available free of charge via the Internet at http://pubs.acs.org.

References and Notes

(1) Mokili, B.; Poitrenaud, C. *Solvent Extr. Ion Exch.* **1996**, *14*, 617.

(2) Katz, J. J.; Seaborg, G. T.; Morss, L. R. *The Chemistry of the Actinide Elements*, 2nd ed.; Chapman and Hall Ltd.: London, 1986.

(3) Spedding, F. H.; Weber, H. O.; Saeger, V. W.; Petheram, H. H.; Rard, J. A.; Habenschuss, A. *J. Chem. Eng. Data* **1976**, *21*, 341.

(4) Rard, J. A.; Weber, H. O.; Spedding, F. H. *J. Chem. Eng. Data* **1977**, *22*, 187.

(5) Rard, J. A.; Shiers, L. E.; Heiser, D. J.; Spedding, F. H. *J. Chem. Eng. Data* **1977**, *22*, 337.

(6) Rard, J. A.; Miller, D. G.; Spedding, F. H. *J. Chem. Eng. Data* **1979**, *24*, 348.

(7) Rard, J. A.; Spedding, F. H. *J. Chem. Eng. Data* **1981**, *26*, 391.

(8) Rard, J. A.; Spedding, F. H. *J. Chem. Eng. Data* **1982**, *27*, 454.

(9) Rard, J. A. *J. Chem. Eng. Data* **1987**, *32*, 92.

(10) Rard, J. A. *J. Chem. Eng. Data* **1987**, *32*, 334.

(11) Smith, R. M.; Martell, A. E. *Critical stability constants*; Plenum Press: New York and London, 1989; Vol. 6, 2nd suppl.

(12) Brönsted, J. N. *J. Am. Chem. Soc.* **1922**, *44*, 877.

(13) Scatchard, G. *Concentrated solutions of strong electrolytes*; Harvard University Press: Cambridge, MA, 1936; Vol. 19, p 309.

(14) Guggenheim, E. A. *Thermodynamics*; North-Holland Publishing Co.: Amsterdam, 1967.

(15) Pitzer, K. S. *J. Phys. Chem.* **1973**, *77*, 268.

(16) Simonin, J. P.; Blum, L.; Turq, P. *J. Phys. Chem.* **1996**, *100*, 7704.

J. Phys. Chem. A, Vol. 110, No. 41, 2006 **11779**

(17) Ruas, A.; Moisy, Ph.; Simonin, J. P.; Bernard, O.; Dufrêche, J. F.; Turq, P. *J. Phys. Chem. B* **2005**, *109*, 5243.

(18) Ruas, A.; Simonin, J. P.; Turq, P.; Moisy, P. *J. Phys. Chem. B* **2005**, *109*, 23043.

(19) Yokoyama, H.; Johansson, G. *Acta Chem. Scand.* **1990**, *44*, 567.

(20) Nelson, D. L.; Irish, D. E. *J. Chem. Soc., Faraday Trans. 1* **1973**, *69*, 156.

(21) Khopkar, P. K.; Narayanankutty, P. *J. Inorg. Nucl. Chem.* **1971**, *33*, 495.

(22) Nelson, D. I.; Irish, D. E. *J. Chem. Phys.* **1971**, *54*, 4479.

(23) Choppin, G. R.; Strazik, W. F. *Inorg. Chem.* **1965**, *4*, 1250.

(24) Bansal, B. M. L.; Patil, S. K.; Sharma, H. D. *J. Inorg. Nucl. Chem.* **1964**, *26*, 993.

(25) Choppin, G. R.; Unrein, P. J. *J. Inorg. Nucl. Chem.* **1963**, *25*, 387.

(26) Rizkalla, E. N.; Choppin, G. R. Lanthanides and actinides hydration and hydrolysis. *Handbook on the Physics and Chemistry of Rare Earths*; Elsevier Science, North-Holland: Amsterdam, 1994; Vol. 18, p 529.

(27) Rogers, R. D. *Lanthanide Actinide Res.* **1987**, *2*, 41.

(28) Spedding, F. H.; Saeger, V. W.; Gray, K. A.; Boneau, P. K.; Brown, M. A.; DeKock, C. W.; Baker, J. L.; Shiers, L. E.; Weber, H. O.; Habenschuss, A. *J. Chem. Eng. Data* **1975**, *20*, 72.

(29) Ravel, B.; Newville, M. *J. Synchrotron Radiat.* **2005**, *12*, 537.

(30) Rehr, J. J.; Albers, R. C. *Rev. Mod. Phys.* **2000**, *72*, 621.

(31) (a) Case, D. A.; et al. *AMBER 6*; University of California: San Francisco, 1999. (b) Cheatham, T. E., III; Cieplak, P.; Kollman, P. A. *J. Biomol. Struct. Dyn.* **1999**, *16*, 845.

(32) Duke, R. E.; Pedersen, L. G. *PMEMD 3.1*; University of North Carolina: Chapel Hill, 2003.

(33) (a) Caldwell, J. W.; Kollman, P. A. *J. Phys. Chem.* **1995**, *99*, 6208. (b) Meng, E. C.; Kollman, P. A. *J. Phys. Chem.* **1996**, *100*, 11460.

(34) Frisch, M. J.; et al. *Gaussian 98*; Gaussian, Inc.: Pittsburgh, PA, 1998.

(35) (a) Dolg, M.; Stoll, H.; Savin, A.; Preuss, H. *Theor. Chim. Acta* **1989**, *75*, 173. (b) Küchle, W.; Dolg, M.; Stoll, H.; Preuss, H. *J. Chem. Phys.* **1994**, *100*, 7535.

(36) Habenschuss, A.; Spedding, F. H. *J. Chem. Phys.* **1979**, *70*, 2797.

(37) Yamagushi, T.; Nomura, N.; Wakita, H.; Ohtaki, H. *J. Chem. Phys.* **1988**, *89*, 5153.

(38) Helm, L.; Merbach, A. E. *Eur. J. Solid State Inorg. Chem.* **1991**, *28*, 245.

(39) Annis, B. K.; Hahn, R. L.; Narten, A. H. *J. Chem. Phys.* **1985**, *82*, 2086.

(40) Yaita, T.; Narita, H.; Suzuki, S.; Tachimori, S.; Motohashi, H.; Shiwaku, H. *J. Radioanal. Nucl. Chem.* **1999**, *239*, 371.

(41) Smith, D. E.; Dang, L. X. *J. Chem. Phys.* **1994**, *100*, 3757.

(42) (a) Sanner, M. F.; Olson, A. J.; Spehner, J. C. *ACM 11th Symposium on Computational Geometry*, Vancouver, BC, Canada, June 5−7, 1995; Association for Computing Machinery: New York, 1995; p C6. (b) Sanner, M. F.; Olson, A. J.; Spehner, J. C. *Biopolymers* **1996**, *38*, 305.

(43) Engler, E.; Wipff, G. MDS, DRAW. In *Crystallography of Supramolecular Compounds*; Tsoucaris, G., Ed.; Kluwer: Dordrecht, The Netherlands, 1996; p 471.

(44) Humphrey, W.; Dalke, A.; Schulten, K. *J. Mol. Graphics* **1996**, *14*, 33.

(45) (a) Waisman, E.; Lebowitz, J. L. *J. Chem. Phys.* **1970**, *52*, 4307. (b) Blum, L. *Mol. Phys.* **1975**, *30*, 1529. (c) Blum, L.; Høye, J. S. *J. Phys. Chem.* **1977**, *81*, 1311. (d) Hiroike, K. *Mol. Phys.* **1977**, *33*, 1195.

(46) Bernard, O.; Blum, L. *J. Chem. Phys.* **1996**, *104*, 4746.

(47) (a) Kalyuzhnyi, Yu V.; Holovko, M. F.; Haymet, A. D. J. *J. Chem. Phys.* **1991**, *95*, 9151. (b) Kalyuzhnyi, Yu V.; Vlachy, V. *Chem. Phys. Lett.* **1993**, *215*, 518. (c) Kalyuzhnyi, Yu V.; Holovko, M. F. *Mol. Phys.* **1993**, *80*, 1165. (d) Holovko, M. F.; Kalyuzhnyi, Yu V. *Mol. Phys.* **1991**, *73*, 1145. (e) Blum, L.; Holovko, M. F.; Protsykevytch, I. A. *J. Stat. Phys.* **1996**, *84*, 191.

(48) Kunz, W.; M'Halla, J.; Ferchiou, S. *J. Phys.: Condens. Matter* **1991**, *3*, 7907.

(49) Simonin, J. P. *J. Phys. Chem. B* **1997**, *101*, 4313.

(50) Simonin, J. P.; Bernard, O.; Blum, L. *J. Phys. Chem. B* **1998**, *102*, 4411.

(51) Ruas, A.; Bernard, O.; Caniffi, B.; Simonin, J. P.; Turq, P.; Blum, L.; Moisy, P. *J. Phys. Chem. B* **2006**, *110*, 3435.

(52) Bernard, O.; Blum, L. *J. Chem. Phys.* **2000**, *112*, 7227.

(53) Lee, L. L. *J. Mol. Liq.* **2000**, *87*, 129.

(54) Spedding, F. H.; Shiers, L. E.; Brown, M. A.; Derer, J. L.; Swanson, D. L.; Habenschuss, A. *J. Chem. Eng. Data* **1975**, *20*, 81.

(55) Spedding, F. H.; Shiers, L. E.; Brown, M. A.; Baker, J. L.; Guitierrez, L.; McDowell, L. S.; Habenschuss, A. *J. Phys. Chem.* **1975**, *79*, 1087.

(56) Libus, Z.; Sadowska, T.; Trzaskowski, J. *J. Chem. Thermodyn.* **1979**, *11*, 1151.

(57) Silber, H. B.; Bakhshandehfar, R.; Contreras, L. A.; Gaizer, F.; Gonsalves, M.; Ismail, S. *Inorg. Chem.* **1990**, *29*, 4473.

(58) Silber, H. B. *Inorg. Chim. Acta* **1987**, *139*, 33.

(59) Johansson, G.; Wakita, H. *Inorg. Chem.* **1985**, *24*, 3047.

(60) Breen, P. J.; Horrocks, W. D., Jr. *Inorg. Chem.* **1983**, *22*, 536.

(61) Bünzli J. C. G.; Yersin J. R. *Inorg. Chem.* **1979**, *18*, 605.

(62) Cossy, C.; Barnes, A. C.; Enderby, J. E.; Merbach, A. E. *J. Chem. Phys.* **1989**, *90*, 3254.

(63) Yamagushi, T.; Tanaka, S.; Wakita, H.; Misawa, M.; Okada, I.; Soper, A. K.; Howells, W. S. *Z. Naturforsch.* **1991**, *46a*, 84.

(64) Johansson, G.; Yokoyama, H. *Inorg. Chem.* **1990**, *29*, 2460.

(65) David, F. H.; Fourest, B. *New J. Chem.* **1997**, *21*, 167.

(66) Luo, Y. R.; Byrne, R. H. *J. Solution Chem.* **2001**, *30*, 837.

(67) Bonal, C.; Morel, J. P.; Morel-Desrosiers, N. *J. Chem. Soc., Faraday Trans.* **1998**, *94*, 1431.

(68) Chen, Z.; Detellier, C. *J. Solution Chem.* **1992**, *21*, 941.

(69) Silber, H. B.; Strozier, M. S. *Inorg. Chim. Acta* **1987**, *128*, 267.

(70) Mironov, V. E.; Avramenko, N. I.; Koperin, A. A.; Blokin, V. V.; Eike, M. Yu; Isayev, I. D. *Koord. Khim.* **1982**, *8*, 636.

(71) Cheung, A. S. C.; Irish, D. E. *J. Inorg. Nucl. Chem.* **1981**, *43*, 1383.

(72) Majdan, M.; Sadowski, P. *Monatsch. Chem.* **1992**, *123*, 987.

(73) Wood, S. A. *Chem. Geol.* **1990**, *82*, 159.

(74) Millero, F. J. *Geochim. Cosmochim. Acta* **1992**, *56*, 3123.

(75) Haas, J. R.; Shock, E. L.; Sassani, D. C. *Geochim. Cosmochim. Acta* **1995**, *59*, 4329.

(76) (a) Binnemans, K.; Görller-Walrand, C. *Chem. Phys. Lett.* **1995**, *235*, 163. (b) Carnall, W. T.; Goodman, G. L.; Rajnak, K. C.; Rana, R. S. *J. Chem. Phys.* **1989**, *90*, 3443. (c) Peijzel, P. S.; Meijerink, A.; Wegh, R. T.; Reid, M. F.; Burdick, G. W. *J. Solid State Chem.* **2005**, *178*, 448.

(77) (a) Freed, S. *Rev. Mod. Phys.* **1942**, *14*, 105. (b) Moulin, C.; Steiner, V.; Plancque, G.; Amekraz, B.; Ansoborlo, E. *Appl. Spectrosc.* **2003**, *57*, 1151. (c) Colette, S.; Amekraz, B.; Madic, C.; Berthon, L.; Cote, G.; Moulin, C. *Inorg. Chem.* **2004**, *43*, 6745.

(78) Kimura, T.; Kato, Y. *J. Alloys Compd.* **1995**, *225*, 284.

(79) Enderby, J. E.; Cummings, S.; Herdman, G. J.; Neilson, G. W.; Salmon, P. S.; Skipper, N. *J. Phys. Chem.* **1987**, *91*, 5851.

(80) Lis, S.; Choppin, G. R. *Mater. Chem. Phys.* **1992**, *31*, 159.

(81) Clavaguéra-Sarrio, C.; Brenner, V.; Hoyau, S.; Marsden, C. J.; Millié, P.; Dognon, J. P. *J. Phys. Chem. B* **2003**, *107*, 3051.